

Thiol-Functionalized IGEPAL[®] Surfactants as Novel Fluorescent Ligands for the Silica Coating of Gold Nanoparticles

Helena Gavilán-Rubio,^[a] João Paulo Coelho,^[a] Guillermo González-Rubio,^[a] Gloria Tardajos,^[a] José Osío Barcina,^[b] Castor Salgado,^[b] and Andrés Guerrero-Martínez*^[a]

Abstract: A synthesized thiol-functionalized non-ionic surfactant based on the IGEPAL[®] (polyoxyethylene(5) nonyl phenyl ether) structure, has been used to replace citrate ions from the surface of gold nanoparticles with 13.5 nm diameters. Upon IGEPAL[®]-type stabilization in water, the nanoparticles were transferred to ethanol, where a layer of silica was efficiently grown on the nanocrystal surface

Keywords: gold · nanomaterials · surfactants

through the conventional Stöber approach. This method allows fine control over the silica thickness, showing uniform and homogeneous core-shell nanoparticles. Additionally, the luminescent properties of the IGEPAL[®] surfactant allow the versatile preparation of robust fluorescent nanoparticles with multiplexing potential as simultaneous plasmonic and fluorescence probes.

1. Introduction

The design of new chemical stabilizers is a driving force in the broad field of colloid science. Such stabilizers could be the answer to physicochemical challenges encountered during the synthesis and use of colloidal particles, such as low stabilities and high tendencies to aggregate.^[1] The synthesis of core-shell architectures is a methodology successfully employed in a “bottom up” approach, which has been efficiently used to overcome these limitations. Within this context, the coating of colloidal nanoparticles with inorganic silica has been frequently studied in materials science for the enhancement of colloidal stability.^[2] Notable examples include the silica coating of colloidal systems for nanoscale metals,^[3] semiconductors,^[4] and magnetic nanoparticles.^[5]

The use of silica as a coating material for colloids is motivated mainly by its high stability^[6] – especially in polar solvents – the easy regulation of the coating process,^[7] the chemical inertness,^[8] and the characteristic optical transparency in the visible spectrum range.^[9] There are mainly two factors favoring the remarkable stability of silica-coated colloids: (i) the van der Waals interactions among silica nanoparticles are much lower than those involving other colloids, as a consequence of the low value of the Hamaker constant;^[10] and (ii) cations and positively charged molecules can be easily attached to the characteristic polymeric silica layer at silica-water interfaces under basic conditions.^[11] Therefore, this silicate layer can confer both steric and electrostatic protection on different cores and act as a dispersing agent of many electrostatic

colloids.^[2] These advantages render silica an ideal, low-cost material to tailor surface properties. Additionally, this coating should endow the cores with several beneficial properties, such as the possibility of subsequent functionalization and biocompatibility,^[1] which allow the use of these nanomaterials to enhance both diagnostic and therapeutic techniques.^[12] Within this context, owing to the optical transparency of silica, this coating material is used as a host matrix for highly luminescent dye molecules that fit inside the porous structure.^[2] These organic dyes are usually inserted after the silica coating by an additional step of synthesis, leading to non-desired aggregation processes that significantly decrease the quantum yields of the fluorophores. Therefore, the discovery of new luminescent ligands that are present during the silica coating process and whose photophysical properties do

[a] H. Gavilán-Rubio, J. P. Coelho, G. González-Rubio, G. Tardajos, A. Guerrero-Martínez
Departamento de Química Física I
Universidad Complutense de Madrid
Avda. Complutense s/n
28040 Madrid (Spain)
e-mail: aguerrero@quim.ucm.es

[b] J. O. Barcina, C. Salgado
Departamento de Química Orgánica I
Universidad Complutense de Madrid
Avda. Complutense s/n
28040 Madrid (Spain)

not undergo significant modification is especially appealing.

A number of reports have been devoted to silica coating of colloidal metal nanoparticles (NPs) by aqueous classical methods, such as Stöber synthesis,^[13] use of silane coupling agents,^[14] and sodium silicate water-glass methodology.^[15] This interest is based on the relevant optical properties that noble metals, such as gold and silver, exhibit at the nanoscale, due to the excitation of the localized surface plasmon resonance (LSPR).^[16] This optical response can be tuned by changing different parameters such as the size, shape, and composition of the NP.^[17] Additionally, the LSPRs of NPs are extremely sensitive to modifications of the local refractive index,^[18] a property that is particularly attractive for sensing applications in nanoplasmonics.^[19] The selection of a suitable silica coating method is mainly determined by the chemical affinity of the metal colloid surface for silica, as well as by the stability of the particles in the coating reaction medium. Interestingly, surface modification with amphiphilic stabilizers greatly assists the transfer of nanoparticles from water into various solvents,^[7,9] such as alcohols, where silica coating can be achieved through controlled hydrolysis and condensation of silanes.^[13–15]

The most successful methods for silica coating of NPs involve prior colloidal stabilization by polymers or surfactants, due to the amphiphilic properties of these chemical species.^[2] Among them, thiol-modified poly(ethylene glycol) polymers have been efficiently used to replace standard capping agents from the surface of NPs to control the direct growth of silica on the particle surfaces through the standard Stöber process.^[9] The combination of the high affinity of thiol groups for metal surfaces^[20] and the non-charged hydrophilic environment that oxyethylene groups offer in aqueous media renders this polymer ideal for silica coating purposes. In relation to poly(ethylene glycol) polymers, IGEPAL[®] surfactants (polyoxyethylene nonyl phenyl ethers),^[21] have been used to generate preferred sites for silica nucleation and growth, due to the strong interaction that ether groups exhibit with silanes through hydrogen bonding.^[22] Additionally, these surfactants are very suitable because they present well-differentiated structural patterns, which offer a way to understand the effect of the chemical structure on their amphiphilic properties.^[23] As a general rule, it has been observed that the critical micelle concentration and the cloud-point temperature of these molecules decrease with shortening of the oxyethylene chain, which is explained in terms of a lower hydrophilic tail hydration, which favors the formation of large aggregates.^[24] Moreover, IGEPAL[®] surfactants have shown interesting photophysical properties that strongly depend on the hydrophobic environment in which the phenyl moiety is immersed during aggregation processes.^[25]

With all this in mind, we report the synthesis of a new thiolated IGEPAL[®]-type surfactant (IgeSH) based on the

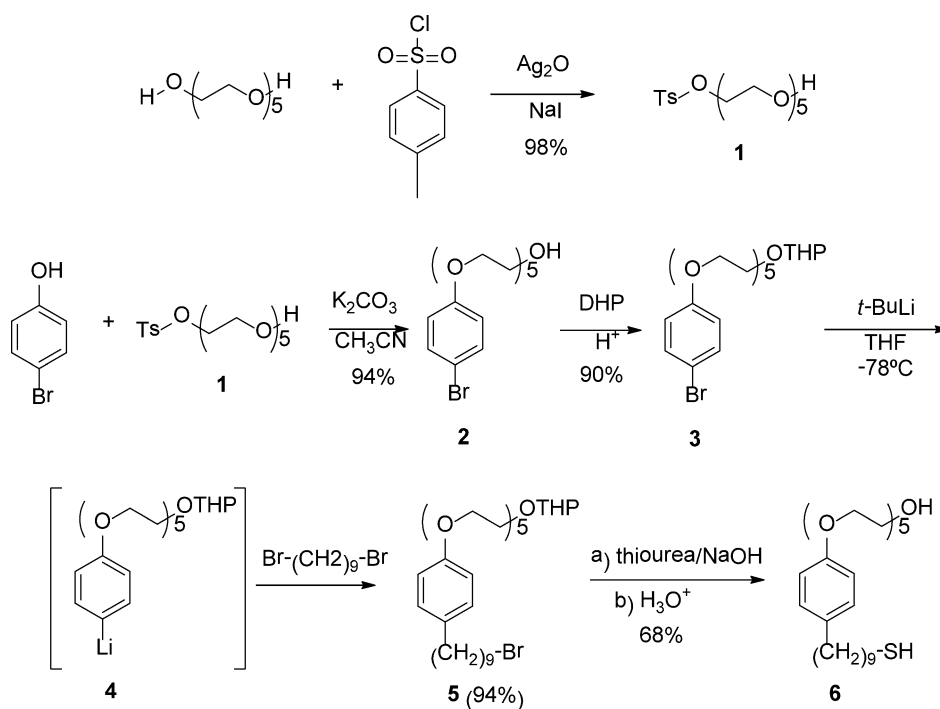
pentaoxyethylene nonyl phenyl ether structure, in which the thiol group has been introduced on the alkyl chain on the opposite side of the phenyl group to ensure coordination to the surface of previously synthesized gold nanoparticles (AuNPs). Using this surfactant, we present a rapid, simple strategy that can be applied to coat AuNPs with homogeneous silica shells (Au@SiO₂NPs) and that allows control over shell thickness. The methodology involves the transfer of AuNPs to ethanol, where silica can be directly condensed on the nanoparticle surface by using the standard Stöber synthesis. Moreover, the luminescent properties of IGEPAL[®]-type surfactants offers a straightforward method to obtain robust fluorescent Au@SiO₂NPs, without the need for further incorporation of fluorophores during the silica growth.^[12]

2. Results and Discussion

Synthesis of the thiol-functionalized IGEPAL[®]-type surfactant. The synthesis of IgeSH (**6**) was carried out following our optimization of a procedure described elsewhere (Scheme 1),^[26] in which the yield was improved. In short, for the preparation of the monotosylate **1**, a modification of the method reported by Bouzide et al. was employed.^[27] Thus, an improved yield of **1** (98% vs. 78%) was obtained using a stoichiometric quantity of NaI instead of catalytic KI. Under these reaction conditions, the amount of the corresponding ditosylate formed as by-product in the reaction was almost negligible.^[28] The reason for this behavior is the stability of the podand-cation complex formed as an intermediate in the reaction, which is greater in the case of pentaethyleneglycol-Na⁺ than with K⁺. Selective monotosylation can be explained by the different acidity of hydrogen atoms H_a and H_b in the complex.

Synthesis and stabilization of AuNPs. In a typical synthesis of spherical AuNPs stabilized with citrate,^[29] a solution of HAuCl₄ was heated to boiling. Then, a solution of sodium citrate was quickly injected into the above solution under vigorous stirring. The mixture was kept boiling until the color changed to red. Then, at room temperature, the mixture was centrifuged to remove the excess of sodium citrate and the precipitate was redispersed in the same volume of water. The resulting citrate-stabilized AuNPs presented a diameter of 13.5 ± 1.5 nm as determined from TEM micrographs (Figure 1).

Then, an aqueous solution of IgeSH was added to the citrate AuNPs solution and stirred overnight. The citrate ions were subsequently replaced by IgeS⁻, a process driven by the stronger interaction of thiol groups with the gold surface (IgeS-AuNPs).^[20] The excess free IgeSH was removed from the solution by centrifugation and redispersion in ethanol. By TEM, no significant differences in the size of IgeS-AuNPs were observed with respect to the initial citrate AuNPs. The replacement of citrate ions by



Scheme 1. Chemical synthesis of the surfactant IgeSH (**6**).

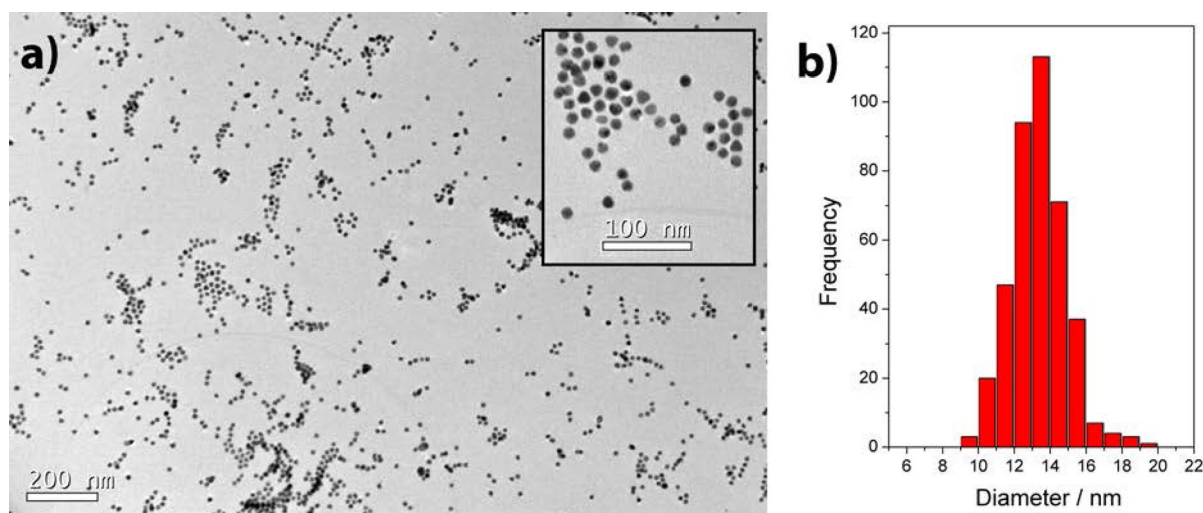


Figure 1. (a) Representative TEM micrographs and (b) size distribution of citrate AuNPs.

the surfactant at the surface of the NPs was followed by zeta potential measurements, which showed a decrease from -30 ± 2 mV to -15 ± 2 mV, which is in good agreement with the zeta potential values of AuNPs coated by polyethylene glycol polymers with low molecular weights.^[30]

For a 2×10^{-10} M solution of IgeS-AuNPs, the final concentration of capping surfactant at the surface of the nanocrystal was estimated at 1.2×10^{-6} M from the UV/Vis spectrum of the supernatants, employing the calculated molar absorptivity of IgeSH at 278 nm in water ($\epsilon_{278} =$

$3.1 \times 10^3 \text{ L mol}^{-1} \text{ cm}^{-1}$).^[26] From this concentration and considering an available surface of 573 nm^2 for a AuNP of 13.5 nm in diameter, the concentration of capping agent around a nanocrystal has been estimated at $\sim 4 \times 10^3$. From this geometric consideration, an area per surfactant molecule of 0.14 nm^2 at the NP surface has been determined. Interestingly, this area is considerably lower than that obtained with AuNPs coated with thiol-modified poly(ethylene glycol) polymers (0.25 nm^2 per molecule),^[9] indicating close-packing of IGEAL®-type molecules at the surface of the nanocrystals.

The UV/Vis absorbance spectrum of the final IgeS-AuNPs in ethanol shows two small maxima at 220 and 278 nm (Figure 2a),^[26] which correspond to the typical absorption bands of the IGEPAL[®] unit, and the characteristic LSPR band of AuNPs at 521 nm (Figure 2a). The maximum of the LSPR band is 5 nm red-shifted in comparison to the initial citrate AuNPs. This change in the LSPR maximum is in good agreement with an increase in the local refractive index of the AuNPs after IgeSH binding and subsequent transfer to ethanol.^[9] The final structure of the resulting IgeS-AuNPs resembles the morphology of non-ionic micelles in water with two hydrophobic/hydrophilic regions: the hydrocarbon and aromatic-like core directly attached to the nanocrystal surface and the external hydrophilic oxyethylene layer in direct contact with solvent molecules.^[23]

Silica coating of AuNPs stabilized with the thiol-functionalized IGEPAL[®]-type surfactant. The surface modification of AuNPs by IgeSH molecules has assisted the transfer of the nanocrystals from water into ethanol (Figure 2a), a prerequisite for the silica coating of AuNPs based on the Stöber synthesis.^[13] After cleaning of IgeS-AuNPs, a relatively concentrated aqueous solution of ammonia was added under vigorous stirring, and finally a diluted solution of tetraethyl orthosilicate (TEOS) in ethanol was injected under gentle stirring. Under these conditions, the IgeS-AuNPs can be directly coated with uniform and homogenous silica shells (Au@SiO₂NPs) by careful selection of the ammonia and TEOS concentrations. Whereas at low ratios ($r = [\text{NH}_3]/[\text{TEOS}] = 0.4$) every single IgeS-AuNP is individually coated with a uni-

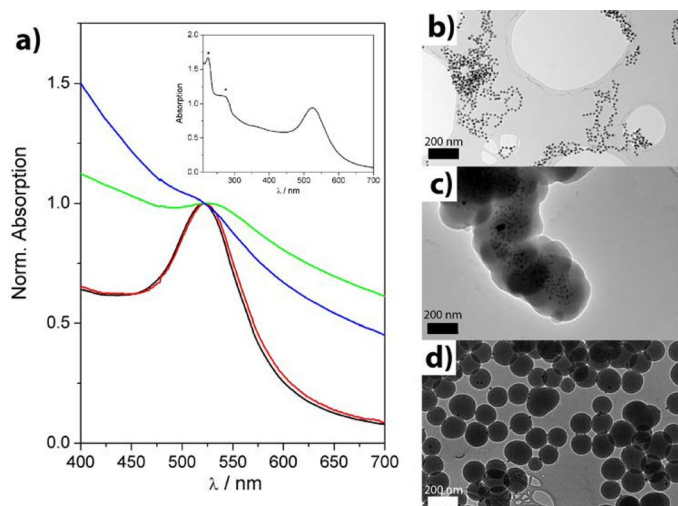


Figure 2. (a) Normalized UV/Vis spectra of the colloids in ethanol, obtained from the silica coating of AuNPs at different concentrations of NH_3 : initial IgeS-AuNPs (black); $[\text{NH}_3] = 0.2$ mM (red); $[\text{NH}_3] = 2.0$ mM (green); and $[\text{NH}_3] = 4.0$ mM (blue). The inset shows the full UV/Vis spectrum of the initial IgeS-AuNPs, where the asterisks show the absorption bands of the ligand. TEM micrographs of AuNPs coated with silica at $[\text{NH}_3] = 0.2$ mM (b), $[\text{NH}_3] = 2.0$ mM (c), and $[\text{NH}_3] = 4.0$ mM (d).

form silica shell (Figure 2b), the increase of r to 2.0 leads to the formation of silica nanoparticles 180 ± 20 nm in diameter, which are decorated by a small fraction of the available IgeS-AuNPs at their surfaces (Figure 2d). At intermediate ratios ($r = 1.0$), uncontrolled aggregation of IgeS-AuNPs within silica nanostructures is observed (Figure 2c). It is noteworthy that at low ratios r the coating with a silica shell as thin as 8.0 ± 1.1 nm (Figures 2a and 3a), which is close to the radius of the AuNPs, was sufficient to render the metal colloids perfectly stable against aggregation.

An advantage of our method over previously reported ones is that it readily provides fine control over the thickness of the silica shells in the critical case of small AuNPs, even for rather thin shells, by simply varying the amount of TEOS added in the initial coating. This is clearly demonstrated by the TEM micrographs in Figure 3a,b, in which r was slightly decreased from 0.4 to 0.2. Thus, a uniform and homogeneous silica layer of 13.1 ± 2.0 nm was easily achieved by slight increase of the TEOS concentration. This result demonstrates the versatility of thiolated IGEPAL[®]-type surfactants as AuNP stabilizers for fine control of thickness of the silica coating in small AuNPs. This ability might be related to the highly dense structure of IGEPAL[®]-type molecules at the surface of the nanocrystal.

Optical properties of silica-coated AuNPs. The effect of the coating on the optical response of the core-shell silica-based nanostructures is shown in Figure 2a. At low ratios r , the LSPR band, initially at 522 nm, red-shifts 2 nm upon silica deposition because of an increase in the local refractive index (from 1.36 in ethanol to 1.46 in amorphous silica) around the AuNPs produced by the

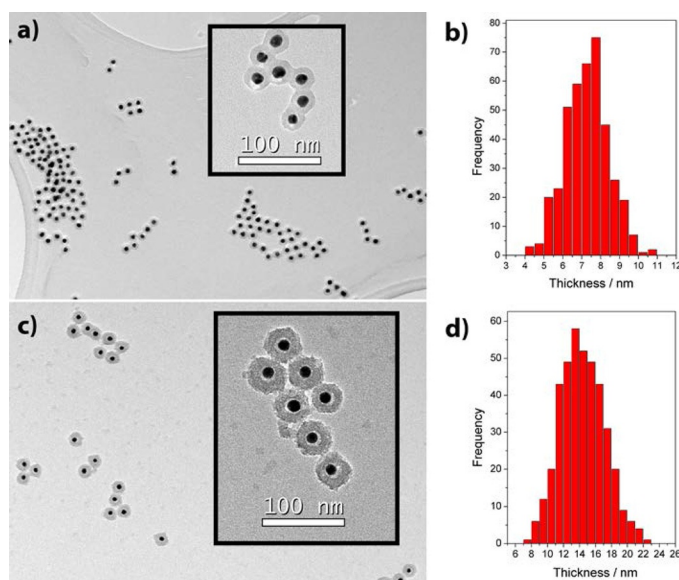


Figure 3. TEM micrographs Au@SiO₂NPs and their respective thickness distributions of the silica layer, at $[\text{NH}_3]/[\text{TEOS}] = 0.4$ (a,b) and 0.2 (c,d), respectively.

silica shell. In contrast, the increase of r to 1.0 leads to a larger shift of the LSPR band (5 nm) and increase of the scattering background, due to the random aggregation of NPs within a thick silica layer. Finally, large values of r induce the formation of large silica NPs that strongly enhance the light scattering background of the UV/Vis spectrum.^[2]

The effect of the silica shell thickness on the optical response of these particles is displayed in Figure 4a. The increase of such thickness from 8.0 to 13.1 nm shifts the LSPR band 4 nm, which supports the idea that the restoring force on the electron oscillation associated with the plasmon mode decreases as the thickness of the silica layer increases.^[31] Therefore, the observed optical effects clearly confirm that there has been absolutely no aggregation during the silica coating at low values of r , unlike the synthesis with high concentrations of ammonia (Figure 2c), pointing to the optimal conditions for the prepara-

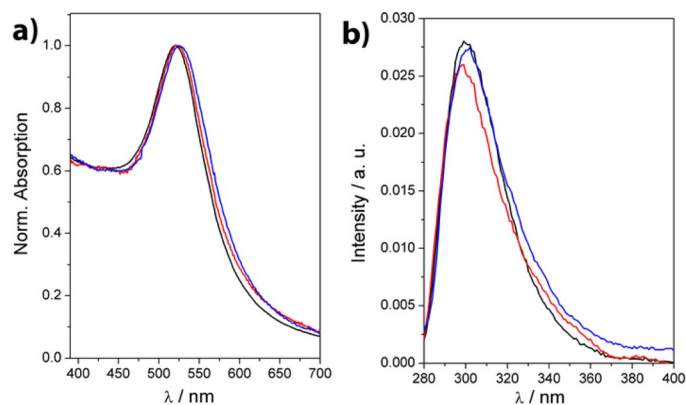


Figure 4. (a) Normalized UV/Vis spectra of the colloids in ethanol, obtained from the silica coating of AuNPs at $[\text{NH}_3]/[\text{TEOS}] = 0.4$ (red) and 0.2 (blue), in comparison to IgeS-AuNPs (black). (b) Emission spectra of equivalent IgeSH (black), IgeS-AuNPs (red), and Au@SiO₂NPs (blue) solutions. The excitation wavelength was fixed at 270 nm.

tion of Au@SiO₂NPs. Additionally, no significant changes in the UV/Vis spectra of Au@SiO₂NPs in ethanol have been observed on the timescale of months, showing the high stability and robustness of the coating material.

Finally, steady-state fluorescence measurements provide detailed information about the luminescent properties of the Au@SiO₂NPs. In their monomeric state, the fluorescence spectrum of IGEPAL[®] surfactants, under excitation at 270 nm, consists of a wide band with a maximum at 299 nm with a typical quantum yield of 0.2.^[25] Analogously, Figure 4b shows the fluorescence spectrum of IgeSH in ethanol at a concentration of 1.0×10^{-6} M, which is the estimated concentration of ligands that is present in a solution of IgeS-AuNPs of concentration 1.6×10^{-10} M. No significant quenching effects have been observed for the equivalent IgeS-AuNP system by com-

parison of the fluorescence spectra, mainly due to the absence of overlapping between the emissive band of IgeSH and the LSPR band of the metal core. Additionally, the emission spectrum of the Au@SiO₂NPs (shell of 13.1 nm thickness) at a concentration of 1.6×10^{-10} M, shows a slight broadness of the emission band with a red shift of 2 nm. These changes suggest a planarization of the aromatic rings at the surface of the AuNPs because of the unfavorable incorporation of the nonpolar aromatic moiety into the negatively charged silica shell, which is in good agreement with the formation of excimers when IGEPAL[®] surfactants aggregate in polar media.^[25] The absence of significant changes in the emission intensity of the Au@SiO₂NPs hints at their multiplexing potential as simultaneous plasmonic and fluorescence probes with quantum yields of ~ 0.2 . Moreover, no changes of the emission intensity have been observed over time, which indicates that the IGEPAL[®] molecules are strongly attached to the gold surface, preventing the release of fluorophores.

3. Conclusions

In summary, we have synthesized a novel thiol functionalized non-ionic surfactant based on the chemical IGEPAL[®] structure to efficiently coat AuNPs with silica. The methodology involves initial aqueous capping ligand replacement, subsequent transfer to ethanol solution, and finally TEOS condensation on the nanocrystal surface through the standard Stöber process. The obtained silica shells are uniform and homogenous, allowing a high degree of control over shell thickness. The corresponding core-shell structures were unambiguously characterized through TEM and UV/Vis spectroscopy. Fluorescence analysis showed that the silica coating of the NPs does not significantly alter the luminescent properties of the IGEPAL[®]-type fluorophores. Thus, we have produced robust plasmonic and fluorescence probes that, after functionalization of the silica surface, may lead to desired biocompatibility; work in this direction is in progress.

4. Experimental Section

4.1 Synthesis and Characterization of the Thiol-Functionalized IGEPAL[®]-Type Surfactant

Materials and methods: All experiments were carried out under argon atmosphere using standard Schlenk techniques. Anhydrous solvents were distilled under argon following standard procedures. Flash chromatography was performed over silica gel 60 (230–400 mesh). All commercially available compounds were purchased from commercial suppliers and used without further purification. The preparation of monotosylate **1** was carried out by modification of a reported procedure.^[1]

Synthesis of monotosylate 1: To a stirred solution of 1.9 g (8 mmol) of pentaerythritol in 50 mL of CH_2Cl_2 at 0 °C, 2.78 g (12 mmol) of Ag_2O , 1.27 g (8.8 mmol) of NaI, and 1.6 g (8.4 mmol) of TsCl were added. The reaction mixture was stirred at room temperature for 20 min, filtered, and washed with 10% NaHCO_3 solution (1 × 25 mL). Evaporation of the solvent, followed by flash chromatography (silica gel, EtOAc) yielded 3.01 g (98%) of **1**. ^1H NMR (300 MHz, $\text{DMSO}-d_6$) δ : 7.79–7.77 (d, 2H), 6.49–6.46 (d, 2H), 4.59 (t, $J=5.4$ Hz, 1H); 4.11 (m, 2H), 3.58–3.55 (m, 2H), 3.49–3.32 (m, 16H) ppm.

Synthesis of compound 2: To a stirred solution of 2.34 g (5.98 mmol) of monotosylate **1** and 1.14 g (6.58 mmol) of *p*-bromophenol in 50 mL of CH_3CN , 909 mg (6.58 mmol) of K_2CO_3 were added. The reaction mixture was refluxed for 48 h, filtered, and concentrated at reduced pressure. The crude product was purified by flash chromatography (silica gel, EtOAc:EtOH=9:1) to yield 2.21 g (94%) of **2**. ^1H NMR (300 MHz, CDCl_3) δ : 7.38–7.29 (m, 2H), 6.83–6.70 (m, 2H), 4.15–4.00 (m, 2H), 3.87–3.78 (m, 2H), 3.74–3.51 (m, 17H) ppm; ^{13}C NMR (75 MHz, CDCl_3) δ : 157.9, 132.3, 116.5, 113.1, 72.5, 70.8, 70.6, 70.5, 70.3, 69.7, 67.7, 61.7 ppm; MS (70 eV): m/z (%): 392 (14) [M^+], 362 (2), 304 (3), 262 (8), 244 (9), 216 (11), 200 (60), 172 (21), 133 (62), 120 (82), 89 (100), 87 (38).

Synthesis of compound 3: A solution of 500 mg (1.27 mmol) of **2**, 214 mg (2.54 mmol) of dihydropyran, and 64 mg (0.25 mmol) of PPTS in 20 mL of CH_2Cl_2 was stirred for 4 h at 25 °C. The reaction mixture was extracted with CH_2Cl_2 (3 × 25 mL), and the organic layer was washed with 10% NaHCO_3 solution (1 × 25 mL) and H_2O (1 × 25 mL) and dried over MgSO_4 . The solvent was evaporated at reduced pressure, and the residue was purified by flash chromatography (silica gel, EtOAc) to afford compound **3** (546 mg, 90%). ^1H NMR (300 MHz, CDCl_3) δ : 7.36–7.30 (m, 2H), 6.80–6.74 (m, 2H), 4.65–4.59 (m, 1H), 4.08 (m, 2H), 3.92–3.80 (m, 4H), 3.74–3.55 (m, 16H), 1.91–1.44 (m, 6H) ppm; ^{13}C NMR (75 MHz, CDCl_3) δ : 157.9, 132.21, 116.5, 113.0, 98.9, 70.9, 70.6, 70.5, 69.6, 67.7, 66.7, 62.2, 30.6, 25.4, 19.5 ppm; MS (70 eV): m/z (%): 478 (10) [$(M+2)^+$], 476 (10) [M^+], 392 (14), 362 (6), 348 (9), 304 (11), 260 (19), 242 (21), 216 (15), 198 (82), 120 (68), 85 (100).

Synthesis of compound 5: 3.8 mL of *t*-BuLi (1.7 M, 6.46 mmol) were slowly added under argon atmosphere at –78 °C to a solution of 1.49 g (3.12 mmol) of **3** in 30 mL of THF. After 5 min, the resulting solution of **4** was added to 3.57 g (12.48 mmol) of 1,9-dibromononane dissolved in 20 mL of THF at –14 °C and stirred at room temperature for 12 h. After addition of 50 mL of water, the reaction mixture was extracted with Et_2O (3 × 30 mL) and dried over MgSO_4 . Evaporation of the solvent and purification of the residue by flash chromatography (silica gel, hexane:EtOAc=9:1) yielded 1.77 g (94%) of **5**. ^1H NMR (300 MHz, CDCl_3) δ : 7.08–7.05 (m, 2H), 6.84–6.80 (m, 2H), 4.63 (m, 1H), 4.19–4.03 (m, 2H), 3.92–3.79 (m,

4H), 3.75–3.43 (m, 16H), 3.40 (t, $J=6.8$ Hz, 2H), 2.58–2.44 (m, 2H), 1.90–1.11 (m, 20H) ppm; ^{13}C NMR (75 MHz, CDCl_3) δ : 156.9, 135.2, 129.3, 114.5, 99.0, 70.9, 70.72, 70.7, 70.6, 69.9, 67.5, 66.7, 62.3, 35.1, 34.1, 32.9, 31.7, 30.6, 29.5, 29.4, 29.2, 28.8, 28.2, 25.5, 19.5 ppm; MS (70 eV): m/z (%): 604 (4) [$(M+2)^+$], 602 (4) [M^+], 518 (87), 474 (4), 440 (7), 386 (8), 342 (14), 324 (30), 298 (5), 177 (9), 151 (14), 133 (37), 107 (68), 85 (100), 73 (30).

Synthesis of compound 6: To a solution of 1.9 g (3.15 mmol) of **5** in 40 mL of ethanol, 259 mg (3.39 mmol) of thiourea were added. The reaction mixture was refluxed for 3 h and cooled to room temperature. A 10% solution of NaOH (2 mL) was added, and the reaction mixture was refluxed for another 2 h. The flask was cooled to 0 °C, acidified to pH 2 with concentrated HCl, and stirred for 24 h at 25 °C. The reaction mixture was extracted with CH_2Cl_2 (3 × 20 mL), and the organic layer was washed with H_2O (1 × 20 mL) and saturated NaCl solution (1 × 25 mL) and dried over MgSO_4 . After evaporation of the solvent, the residue was purified by flash chromatography (silica gel, EtOAc:MeOH=9:1) to obtain 1.02 g (68%) of **6**. ^1H NMR (300 MHz, CDCl_3) δ : 7.08–7.05 (m, 2H), 6.84–6.81 (m, 2H), 4.12–4.09 (m, 2H), 3.86–3.82 (2H, m), 3.74–3.58 (16H, m), 2.79 (1H, m), 2.50 (4H, m), 1.61–1.21 (15H, m) ppm; ^{13}C NMR (75 MHz, CDCl_3) δ : 156.9, 135.4, 129.3, 114.6, 72.7, 70.9, 70.7, 70.4, 69.9, 67.6, 61.8, 35.2, 32.3, 31.8, 29.85, 29.8, 29.6, 29.4, 29.1 ppm; MS (70 eV): m/z (%): 472 (2) [M^+], 438 (2), 394 (2), 340 (2), 311 (4), 283 (7), 246 (7), 220 (6), 177 (10), 135 (12), 133 (75), 107 (100), 89 (63).

4.2 Synthesis and Capping Agent Replacement of AuNPs

Materials and methods: All the starting materials were obtained from commercial suppliers and used without further purification. Sodium citrate, ammonium hydroxide (25% v/v), TEOS, and ethanol (96% v/v) were purchased from Sigma-Aldrich. Tetrachloroauric(III) acid ($\text{HAuCl}_4 \cdot 3\text{H}_2\text{O}$) was supplied by Alfa Aesar. Milli-Q water was used in all preparations (conductivity less than $16 \mu\text{S cm}^{-1}$).

Synthesis of citrate-stabilized AuNPs: In this synthesis, the reduction of chloroauric acid in the presence of sodium citrate takes place, producing size-defined AuNPs. Typically, 2 mL of a 25 mM HAuCl_4 aqueous solution were added to 125 mL of distilled water. The solution was brought to its boiling point. Then, 5 mL of a 1% w/w sodium citrate solution was added under vigorous stirring. In approximately 10 min, a change of color from blackish to red was observed. Once this point was reached, the solution was allowed to cool to room temperature. In order to remove the excess citrate ions, the as-synthesized solution was centrifuged for 90 min at 7500 rpm, and the precipitate was dispersed in distilled water.

Capping agent replacement: Citrate-stabilized AuNPs were transferred from aqueous media into ethanol via

ligand exchange through the thiolated IGEPAL®-type surfactant. Thus, 40 mL of a 0.3 mM IgeSH aqueous solution were added to 10 mL of a 0.5 mM dispersion containing the AuNPs. The exchange reaction was allowed to continue overnight under magnetic stirring. The sample was washed with distilled water and centrifuged for 90 min at 7500 rpm, and the gold concentration was adjusted to 1.8 mM.

4.3 Silica Coating of AuNPs

The silica shells were grown directly by adding 0.405 mL of a 1.8 mM IgeS-AuNPs ethanolic solution to 1 mL of 1:4 v/v H₂O/EtOH solution. The amount of NH₃ was optimized, and the ideal amount for this system was found to be 20 μ L. This precise quantity of base was mixed with the solution and mechanically shaken. Afterwards, 1 mL of this solution was mixed with 60 μ L of an ethanolic solution containing a certain amount of TEOS (typically this solution contained 1.5 mL of EtOH and 10–40 μ L of TEOS). The final concentration of each reagent was: [Au]=0.47 mM, [NH₃]=0.2 mM, [TEOS]=2.5–10 mM (depending upon the desired shell thickness). After the silica precursor was added, the solution was briefly and vigorously shaken, and it was allowed to react for 2 h. The system was then kept undisturbed. The product was collected by centrifugation at 6000 rpm for 150 min, and finally it was redispersed in 300 μ L of EtOH.

4.4 Characterization Techniques

¹H and ¹³C NMR measurements: ¹H and ¹³C NMR spectra were recorded on a Bruker Avance DPX-300 spectrometer (300 MHz, 7.05 T). Chemical shifts are given in ppm relative to TMS (¹H, 0.0 ppm) and CDCl₃ (¹³C, 77.0 ppm). Coupling constants are given in Hertz.

TEM: TEM images were obtained with a JEOL JEM 2100 transmission electron microscope operating at an acceleration voltage of 200 kV.

UV/Vis measurements: UV/Vis absorption spectra were registered using a UVICON XL spectrophotometer (Bio-Tex Instruments). All experiments were carried out at 298 K, using quartz cuvettes with optical paths of 1 cm.

Fluorescence measurements: Steady-state fluorescence spectra were recorded at 298 K using an AMINCO Bowman Series 2 spectrofluorometer, with 4.0 nm bandwidth for excitation and emission and quartz cuvettes with optical paths of 1 cm. The excitation wavelength was fixed at 270 nm.

Electrophoretic mobility: The zeta potential was determined through electrophoretic mobility measurements using a Malvern Zetasizer 2000 instrument.

Acknowledgments

This work has been funded by the *I Convocatoria de Ayudas Fundación BBVA a Investigadores, Innovadores y Creadores Culturales* and the Madrid Regional Government (S2013/MIT-2807). J. P. C. acknowledges receipt of a Ciência sem Fronteiras fellowship from the CNPq of Brazil. A. G.-M. acknowledges receipt of a Ramón y Cajal Fellowship from the Spanish MINECO.

References

- [1] A. Schroedter, H. Weller, *Angew. Chem. Int. Ed.* **2002**, *41*, 3218–3221.
- [2] A. Guerrero-Martínez, J. Pérez-Juste, L. M. Liz-Marzán, *Adv. Mater.* **2010**, *22*, 1182–1195.
- [3] C. Graf, D. L. J. Vossen, A. Imhof, A. van Blaaderen, *Langmuir* **2003**, *19*, 6693–6700.
- [4] Y. Yang, L. Jing, X. Yu, D. Yan, M. Gao, *Chem. Mater.* **2007**, *19*, 4123–4128.
- [5] H. Xu, L. Cui, N. Tong, H. Gu, *J. Am. Chem. Soc.* **2006**, *128*, 15582–15583.
- [6] L. M. Liz-Marzán, M. A. Correa-Duarte, I. Pastoriza-Santos, P. Mulvaney, T. Ung, M. Giersig, N. A. Kotov, in *Handbook of Surfaces and Interfaces of Materials* (Ed.: H. S. Nalwa), Academic Press, San Diego, U.S.A., **2001**.
- [7] I. Pastoriza-Santos, J. Pérez-Juste, L. M. Liz-Marzán, *Chem. Mater.* **2006**, *18*, 2465–2467.
- [8] G. Jianping, Z. Qiao, Z. Tierui, Y. Yadong, *Angew. Chem. Int. Ed.* **2008**, *47*, 8924–8928.
- [9] C. Fernández-López, C. Mateo-Mateo, R. A. Álvarez-Puebla, J. Pérez-Juste, I. Pastoriza-Santos, L. M. Liz-Marzán, *Langmuir* **2009**, *25*, 13894–13899.
- [10] L. Bergström, *Adv. Colloid Interface Sci.* **1997**, *170*, 125–169.
- [11] G. Vigil, Z. Xu, S. Steinberg, J. Israelachvili, *J. Colloid Interface Sci.* **1994**, *165*, 367–385.
- [12] A. Burns, H. Ow, U. Wiesner, *Chem. Soc. Rev.* **2006**, *35*, 1028–1042.
- [13] W. Stöber, A. Fink, E. Bohn, *J. Colloid Interface Sci.* **1968**, *26*, 62–69.
- [14] E. P. Plueddemann, in *Silane Coupling Agents*, Plenum Press, New York, U.S.A., **1991**.
- [15] L. M. Liz-Marzán, M. Gierseig, P. Mulvaney, *Langmuir* **1996**, *12*, 4329–4335.
- [16] U. Kreibitz, M. Vollmer, in *Optical Properties of Metal Clusters*, Springer-Verlag, Berlin, **1996**.
- [17] A. Guerrero-Martínez, M. Grzelczak, L. M. Liz-Marzán, *ACS Nano* **2012**, *6*, 3655–3662.
- [18] H. Chen, T. Ming, L. Zhao, F. Wang, L.-D. Sun, J. Wanga, C.-H. Yan, *Nano Today* **2010**, *5*, 494–505.
- [19] S. Liu, Z. J. Tang, *J. Mater. Chem.* **2010**, *20*, 24–35.
- [20] R. M. Smith, A. E. Martell, in *Critical Stability Constants, Vol. 4: Inorganic Complexes*, Plenum Press, New York, U.S.A., **1976**.
- [21] S. Santra, R. Tapeç, N. Theodoropoulou, J. Dobson, A. Hebard, W. H. Tan, *Langmuir* **2001**, *17*, 2900–2906.
- [22] H. Elimelech, D. Avnir, *Chem. Mater.* **2008**, *20*, 2224–2227.
- [23] G. Tardajos, T. Montoro, M. H. Viñas, M. A. Palafox, Andrés Guerrero-Martínez, *J. Phys. Chem. B* **2008**, *112*, 15691–15700.

- [24] K. Toerne, R. von Wandruszka, *Langmuir* **2002**, *18*, 7349–7353.
- [25] A. Guerrero-Martínez, T. Montoro, M. H. Viñas, G. González-Gaitano, G. Tardajos, *J. Phys. Chem. B* **2007**, *111*, 1368–1376.
- [26] J. P. Coelho, G. González-Rubio, A. Delices, J. Osío Barcina, C. Salgado, D. Ávila, O. Peña-Rodríguez, G. Tardajos, A. Guerrero-Martínez, *Angew. Chem. Int. Ed.* **2014**, *53*, 12751–12755.
- [27] A. Bouzide, G. Sauvé, *Org. Lett.* **2002**, *4*, 2329–12332.
- [28] P. G. M. Wuts, T. W. Greene, in *Protective Groups in Organic Synthesis*, 4th Edition, Wiley, New York, **2012**.
- [29] B. V. Enüstün, J. Turkevich, *J. Am. Chem. Soc.* **1963**, *85*, 3317–3328.
- [30] K. Rahme, L. Chen, R. G. Hobbs, M. A. Morris, C. O. Driscoll, J. D. Holmes, *RSC Adv.* **2013**, *3*, 6085–6094.
- [31] P. Mulvaney, *Langmuir* **1996**, *12*, 788–800.

Received: May 28, 2015

Accepted: June 25, 2015

Published online: August 26, 2015